Supporting information

Synthesis and Characterization of a Series of Model Complexes of the Active Site of [Fe]-Hydrogenase (Hmd)

Dafa Chen,[†] Annegret Ahrens-Botzong,[‡] Volker Schünemann,[‡] Rosario Scopelliti,[†] and Xile Hu*[†]

[†] Laboratory of Inorganic Synthesis and Catalysis
Institute of Chemical Sciences and Engineering
Ecole Polytechnique Fédérale de Lausanne (EPFL)
SB-ISIC-LSCI, BCH 3305, Lausanne, CH 1015, Switzerland

[‡] Fachbereich Physik
Technische Universität Kaiserslautern
D-67663 Kaiserslautern, Germany

* To whom correspondence should be addressed. E-mail: xile.hu@epfl.ch

A. Crystallographic Details for [Fe(CO)$_2$(PPh$_3$)I(hp)] (**2**)

A total of 15689 reflections (-17 $\leq h \leq$ 17, -10 $\leq k \leq$ 10, -24 $\leq l \leq$ 24) were collected at T = 140(2) K in the range of 2.55 to 26.37^o of which 4755 were unique (R_{int} = 0.0220); Mo$_{K\alpha}$ radiation (λ= 0.71073 Å). The structure was solved by the direct methods. All non-hydrogen atoms were refined anisotropically, and hydrogen atoms were placed in calculated idealized positions. The residual peak and hole electron densities were 0.352 and –0.233 eA^{-3}, respectively. The absorption coefficient was 2.056 mm^{-1}. The least squares refinement converged normally with residuals of $R(F)$ = 0.0202, $wR(F^2)$ = 0.0432 and a GOF = 1.014 (I>2σ(I)). C$_{25}$H$_{19}$FeINO$_3$P, Mw = 595.13, space group $P2_1/c$, Monoclinic, a = 14.0180(4), b = 8.8000(2), c = 19.9447(5) Å, β = 107.747(3) ^{o}, V = 2343.26(10) Å^3, Z = 4, ρ_{calcd} = 1.687 Mg/m^3.

B. Crystallographic Details for [Fe(CO)$_2$(PPh$_3$)I(hpp)] (**3**)

A total of 20330 reflections (-14 $\leq h \leq$ 14, -18 $\leq k \leq$ 19, -17 $\leq l \leq$ 18) were collected at T = 140(2) K in the range of 2.91 to 26.02^o of which 5313 were unique (R_{int} = 0.0399); Mo$_{K\alpha}$ radiation (λ= 0.71073 Å). The structure was solved by the direct methods. All non-hydrogen atoms were refined anisotropically, and hydrogen atoms were placed in calculated idealized positions. The residual peak and hole electron densities were 0.845 and –0.339 eA^{-3}, respectively. The absorption coefficient was 1.787 mm^{-1}. The least squares refinement converged normally with residuals of $R(F)$ = 0.0304, $wR(F^2)$ = 0.0657 and a GOF = 0.991 (I>2σ(I)). C$_{31}$H$_{23}$FeINO$_3$P, Mw = 671.22, space group $P2_1/n$, Monoclinic, a = 12.1692(7), b = 15.9364(8), c = 14.6654(9) Å, β = 107.473(6) ^{o}, V = 2712.9(3) Å^3, Z = 4, ρ_{calcd} = 1.643 Mg/m^3.

C. Crystallographic Details for [Fe(CO)$_2$(PEt$_3$)I(hmp)] (**4**)

A total of 14550 reflections (-9 $\leq h \leq$ 9, -17 $\leq k \leq$ 21, -18 $\leq l \leq$ 17) were collected at T = 140(2) K in the range of 2.87 to 27.88^o of which 4094 were unique (R_{int} = 0.0334); Mo$_{K\alpha}$ radiation (λ= 0.71073 Å). The structure was solved by the direct methods. All non-hydrogen atoms were refined anisotropically, and hydrogen atoms were placed in calculated idealized positions. The residual peak and hole electron densities were 0.464 and –0.407 eA^{-3}, respectively. The absorption coefficient was 2.764 mm^{-1}. The least squares refinement converged normally with residuals of $R(F)$ = 0.0246, $wR(F^2)$ = 0.0531 and a GOF = 1.035 (I>2σ(I)). C$_{14}$H$_{21}$FeINO$_3$P, Mw = 465.04, space group $P2_1/n$, Monoclinic, a = 7.49550(10), b = 16.4875(4), c = 14.0187(3) Å, β = 95.2490(17) ^{o}, V = 1725.19(6) Å^3, Z = 4, ρ_{calcd} = 1.790 Mg/m^3.

D. Crystallographic Details for [Fe(CO)$_2$(PPh$_3$)(hmp){S(2-iPr-C$_6$H$_4$)}] (**6**)

A total of 12233 reflections (-13 $\leq h \leq$ 13, -14 $\leq k \leq$ 13, -18 $\leq l \leq$ 18) were collected at T = 140(2) K in the range of 2.77 to 26.02^o of which 6506 were unique (R_{int} = 0.1119); Mo$_{K\alpha}$ radiation (λ= 0.71073 Å). The structure was solved by the direct methods. All non-hydrogen atoms were refined anisotropically, and hydrogen atoms were placed in calculated idealized positions. The residual peak and hole electron densities were 2.170 and –0.974 eA^{-3}, respectively. The absorption coefficient was 0.764 mm^{-1}. The least squares refinement converged normally with residuals of $R(F)$ = 0.1128, $wR(F^2)$ = 0.2409 and a GOF = 0.930 (I>2σ(I)). C$_{36}$H$_{34}$Cl$_2$FeNO$_3$PS, Mw = 718.42, space group P-1, Triclinic, a = 11.0759(19), b = 11.5177(14), c = 15.082(2) Å, α = 71.085(12), β = 78.739(13), γ = 66.159(14) ^{o}, V = 1660.2(4) Å^3, Z = 2, ρ_{calcd} = 1.437 Mg/m^3.

E.   Crystallographic Details for [Fe(CO)$_2$(PPh$_3$)(hmp){S(2,4,6-Me$_3$C$_6$H$_2$)}]] (**7**)

A total of 7201 reflections (-20 $\leq h \leq$ 19, -18 $\leq k \leq$ 18, -18 $\leq l \leq$ 19) were collected at $T = 100(2)$ K in the range of 3.38 to 27.54° of which 7201 were unique (R_{int} = 0.0000); Mo$_{K\alpha}$ radiation (λ= 0.71073 Å). The structure was solved by the direct methods. All non-hydrogen atoms were refined anisotropically, and hydrogen atoms were placed in calculated idealized positions. The residual peak and hole electron densities were 1.150 and –0.464 eA^{-3}, respectively. The absorption coefficient was 0.634 mm^{-1}. The least squares refinement converged normally with residuals of $R(F)$ = 0.0653, $wR(F^2)$ = 0.1390 and a GOF = 1.191 (I>2$\sigma(I)$). C$_{35}$H$_{32}$FeNO$_3$PS, Mw = 633.50, space group $P2_1/c$, Monoclinic, a = 15.649(3), b = 13.890(2), c = 14.8057(13) Å, β = 102.833(10) °, V = 3137.9(8) Å^3, Z = 4, ρ_{calcd} = 1.341 Mg/m^3.

F.   Crystallographic Details for *cis*-(I, PPh$_3$)-Fe(CO)$_2$(PPh$_3$)I(OMe-PyS) (**10a**)

A total of 43518 reflections (-11 $\leq h \leq$ 11, -25 $\leq k \leq$ 25, -22 $\leq l \leq$ 22) were collected at T = 100(2) K in the range of 3.09 to 27.50 ° of which 6737 were unique (R_{int} = 0.0947); Mo$_{K\alpha}$ radiation (λ= 0.71073 Å). The structure was solved by the direct methods. All non-hydrogen atoms were refined anisotropically, and hydrogen atoms were placed in calculated idealized positions. The residual peak and hole electron densities were 2.401 and –2.651 eA^{-3}, respectively. The absorption coefficient was 1.885 mm^{-1}. The least squares refinement converged normally with residuals of $R(F)$ = 0.0619, $wR(F^2)$ = 0.1595 and a GOF = 1.302 (I>2$\sigma(I)$). C$_{26}$H$_{21}$FeINO$_3$PS•CH$_2$Cl$_2$, Mw = 726.14, space group $P2_1/c$, Monoclinic, a = 8.7884(8), b = 19.780(2), c = 17.558(3) Å, β = 103.934(8)°, V = 2962.3(7) Å^3, Z = 4, ρ_{calcd} = 1.628 Mg/m^3.

G.   Crystallographic Details for *trans*-(I, PPh$_3$)-Fe(CO)$_2$(PPh$_3$)I(OMe-PyS) (**10b**)

A total of 23989 reflections (-10 $\leq h \leq$ 10, -16 $\leq k \leq$ 16, -17 $\leq l \leq$ 17) were collected at T = 100(2) K in the range of 3.06 to 25.00 ° of which 5759 were unique (R_{int} = 0.0854); Mo$_{K\alpha}$ radiation (λ= 0.71073 Å). The structure was solved by the direct methods. All non-hydrogen atoms were refined anisotropically, and hydrogen atoms were placed in calculated idealized positions. The residual peak and hole electron densities were 1.395 and –0.632 eA^{-3}, respectively. The absorption coefficient was 1.700 mm^{-1}. The least squares refinement converged normally with residuals of $R(F)$ = 0.0807, $wR(F^2)$ = 0.1879 and a GOF = 1.323 (I>2$\sigma(I)$). C$_{26}$H$_{21}$FeINO$_3$PS•CH$_2$Cl$_2$, Mw = 726.14, space group P-1, Triclinic, a = 8.7114(15), b = 14.042(3), c = 15.126(3) Å, α = 109.470(17), β = 92.157(15), γ = 107.654(14)°, V = 1642.4(5) Å^3, Z = 2, ρ_{calcd} = 1.468 Mg/m^3.

H.   Crystallographic Details for [Fe(CO)$_2$(PPh$_3$)$_2${S(6-Me-C$_5$H$_3$N)}]$^+$(PF$_6$)$^-$·3CH$_3$CN (**11**)

A total of 21507 reflections (-14 $\leq h \leq$ 14, -18 $\leq k \leq$ 18, -18 $\leq l \leq$ 18) were collected at T = 140(2) K in the range of 2.85 to 26.02 ° of which 9450 were unique (R_{int} = 0.0305); Mo$_{K\alpha}$ radiation (λ= 0.71073 Å). The structure was solved by the direct methods. All non-hydrogen atoms were refined anisotropically, and hydrogen atoms were placed in calculated idealized positions. The residual peak and hole electron densities were 0.400 and –0.286 eA^{-3}, respectively. The absorption coefficient was 0.522 mm^{-1}. The least squares refinement converged normally with residuals of $R(F)$ = 0.0441, $wR(F^2)$ = 0.0983 and a GOF = 1.037 (I>2$\sigma(I)$). C$_{50}$H$_{45}$F$_6$FeN$_4$O$_2$P$_3$S, Mw = 1028.72, space group P-1, Triclinic, a = 11.6427(3), b = 14.8175(5), c = 14.9136(5) Å, α = 76.110(3), β = 76.397(3), γ = 81.470(3)°, V = 2416.00(14) Å^3, Z = 2, ρ_{calcd} = 1.414 Mg/m^3.

I. Crystallographic Details for [Fe(CO)$_2$I(2,6-Me$_2$C$_6$H$_3$NC)(SC$_5$H$_4$N-CO)] (13)

A total of 14104 reflections ($-9 \leq h \leq 9$, $-22 \leq k \leq 22$, $-17 \leq l \leq 17$) were collected at $T = 140(2)$ K in the range of 2.72 to 26.37 $^{\circ}$ of which 3751 were unique (R$_{int}$ = 0.0568); Mo$_{K\alpha}$ radiation (λ= 0.71073 Å). The structure was solved by the direct methods. All non-hydrogen atoms were refined anisotropically, and hydrogen atoms were placed in calculated idealized positions. The residual peak and hole electron densities were 3.010 and -1.176 eA^{-3}, respectively. The absorption coefficient was 2.612 mm^{-1}. The least squares refinement converged normally with residuals of $R(F)$ = 0.0567, $wR(F^2)$ = 0.1521 and a GOF = 1.020 ($I>2\sigma(I)$). C$_{17}$H$_{13}$FeIN$_2$O$_3$S, Mw = 508.10, space group $P2_1/n$, Monoclinic, a = 7.5304(9), b = 17.855(2), c = 13.8288(15) Å, β = 95.161(10)°, V = 1851.8(4) Å^3, Z = 4, ρ_{calcd} = 1.823 Mg/m^3.
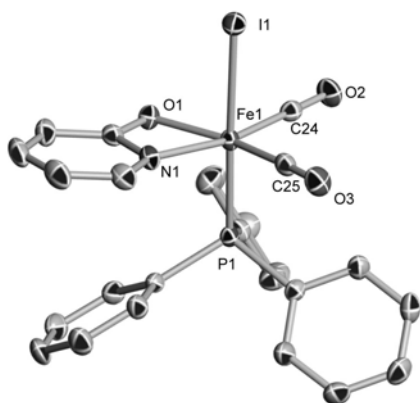
Figure S1. Solid-state structure of **2**. The thermal ellipsoids are displayed in 50% probability. Selected bond distances (Å) and angles (°): Fe1-N1, 1.9575(16); Fe1-O1, 2.0274(13); Fe1-P1, 2.2556(6); Fe1-C24, 1.794(2); Fe1-C25, 1.778(2); Fe1-I1, 2.6536(3); C24-O2, 1.136(2); C25-O3, 1.140(2); C5-O1, 1.309(2); C5-N1, 1.349(2); C1-N1, 1.342(3); C24-Fe1-C25, 94.74(9); O1-Fe1-N1, 66.42(6).
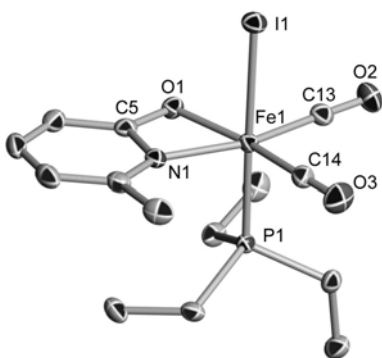

Figure S2. Solid-state molecular structure of complex **4**. The thermal ellipsoids are displayed at 50% probability. Selected bond distances (Å) and angles (°): Fe1-N1, 1.973(2); Fe1-O1, 2.0104(16); Fe1-P1, 2.2477(6); Fe1-C13, 1.787(3); Fe1-C14, 1.774(2); Fe1-I1, 2.6752(3); C13-O2, 1.135(3); C14-O3, 1.140(3); C5-O1, 1.307(3); C5-N1, 1.355(3); C13-Fe1-C14, 90.57(11); O1-Fe1-N1, 66.63(7).
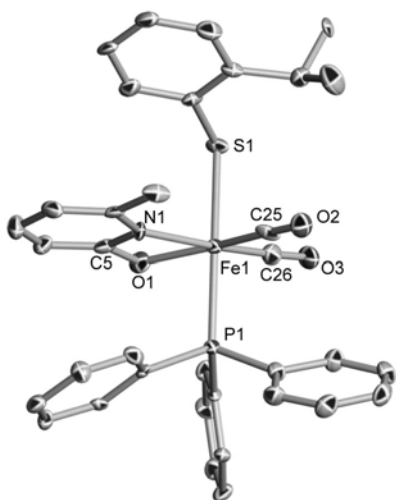
Figure S3. Solid-state molecular structure of complex **6**. The thermal ellipsoids are displayed at 50% probability. Selected bond distances (Å) and angles (^{o}): Fe1-N1, 1.967(8); Fe1-O1, 2.001(6); Fe1-P1, 2.273(3); Fe1-C25, 1.808(11); Fe1-C26, 1.812(10); Fe1-S1, 2.365(3); C25-O2, 1.128(10); C26-O3, 1.123(10); C5-O1, 1.323(12); C5-N1, 1.373(12); C25-Fe1-C26, 93.6(4); O1-Fe1-N1, 67.3(3).
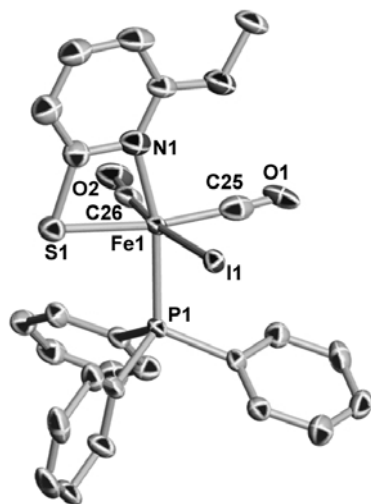

Figure S4. Solid-state molecular structure of complex **10a**. The thermal ellipsoids are displayed at 50% probability. One CH_2Cl_2 molecule was omitted. Selected bond distances (Å) and angles (^{o}): Fe1-I1, 2.6716(9); Fe1-N1, 2.002(6); Fe1-P1, 2.2769(16); Fe1-C25, 1.823(9); Fe1-C26, 1.788(6); Fe1-S1, 2.3888(19); C25-O1, 1.021(9); C26-O2, 1.135(8); C25-Fe1-C26, 89.8(3).
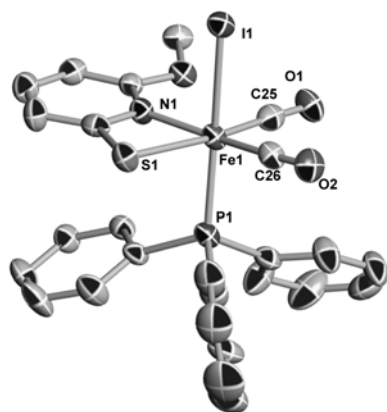
Figure S5. Solid-state molecular structure of complex **10b**. The thermal ellipsoids are displayed at 50% probability. One CH_2Cl_2 molecule was omitted. Selected bond distances (Å) and angles (^{o}): Fe1-I1, 2.6777(16); Fe1-N1, 2.005(8); Fe1-P1, 2.257(3); Fe1-C25, 1.784(13); Fe1-C26, 1.790(11); Fe1-S1, 2.365(3); C25-O1, 1.167(13); C26-O2, 1.134(12); C25-Fe1-C26, 90.3(5).
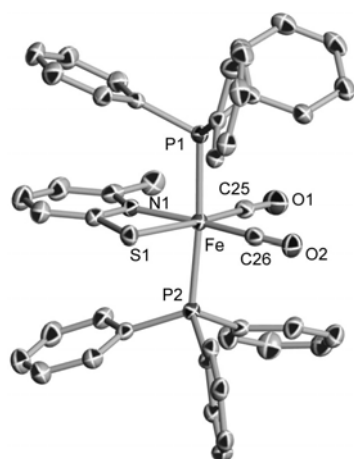

Figure S6. Solid-state molecular structure of complex **11**. The thermal ellipsoids are displayed at 50% probability. Selected bond distances (Å) and angles (^{o}): Fe1-N1, 1.997(2); Fe1-P1, 2.3146(8); Fe1-P2, 2.3045(8); Fe1-C25, 1.807(3); Fe1-C26, 1.779(3); Fe1-S1, 2.3322(8); C25-O2, 1.131(3); C26-O3, 1.144(3); C25-Fe1-C26, 89.58(12).
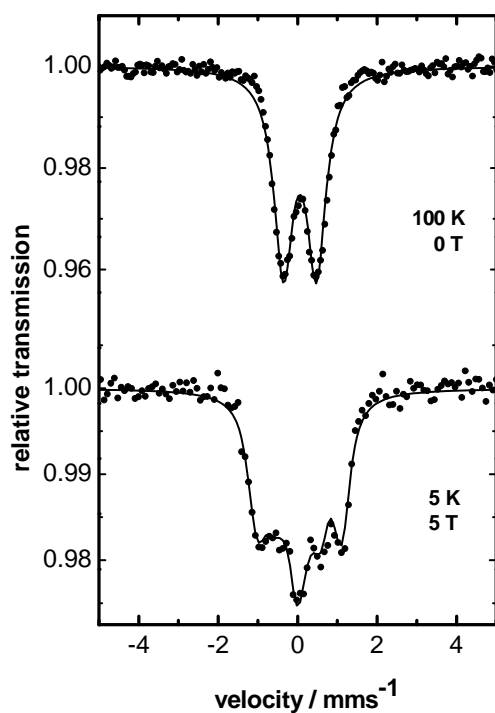
Fig. S7. (Top) Mössbauer spectrum of complex **5** taken at 100 K. The isomer shift is δ = 0.06 ($\pm$0.02) mms^{-1}, the quadrupole splitting is ΔE_Q = (-) 0.83 ($\pm$0.02) mms^{-1} and the linewidth is Γ = 0.58 ($\pm$0.02) mms^{-1}. (Bottom) Mössbauer spectrum of complex **5** taken at 5 K with a magnetic field of 5 T perpendicular to the γ-ray. The isomer shift is δ = 0.04 ($\pm$0.02) mms^{-1}, the quadrupole splitting is ΔE_Q = - 0.87 ($\pm$0.03) mms^{-1} and the linewidth is Γ = 0.44 ($\pm$0.02) mms^{-1}.
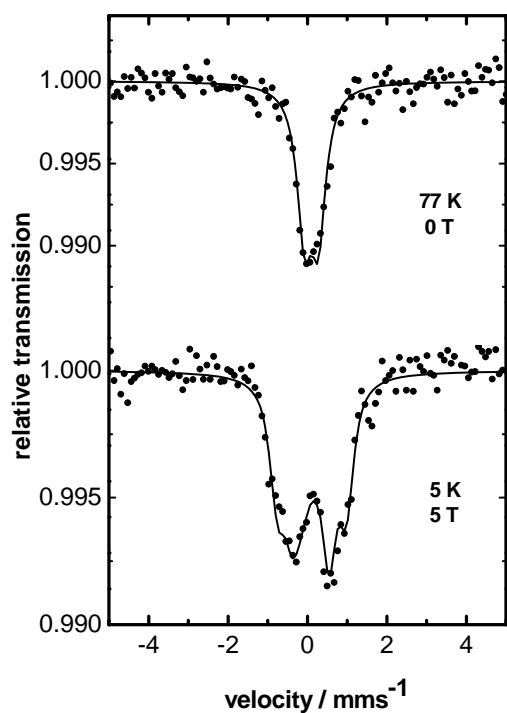
Fig. S8. (Top) Mössbauer spectrum of complex **9** taken at 77 K. The isomer shift is $\delta = 0.10$ (± 0.01) mms^{-1}, the quadrupole splitting is $\Delta E_Q = -0.35$ (± 0.03) mms^{-1} and the linewidth is $\Gamma = 0.45$ (± 0.05) mms^{-1}. (Bottom) Mössbauer spectrum of complex **9** taken at 5 K with a magnetic field of 5 T perpendicular to the γ-ray. The isomer shift is $\delta = 0.11$ (± 0.02) mms^{-1}, the quadrupole splitting is $\Delta E_Q = -0.36$ (± 0.03) mms^{-1} and the linewidth is $\Gamma = 0.40$ (± 0.02) mms^{-1}.
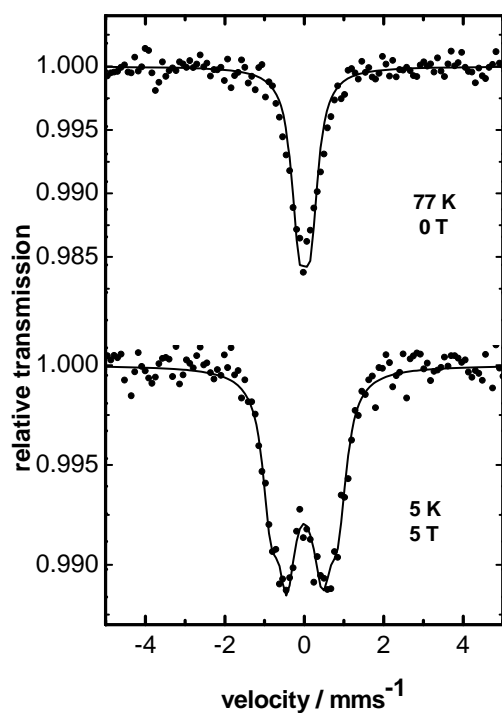
Fig. S9. (Top) Mössbauer spectrum of complex **13** taken at 77 K. The isomer shift is $\delta = 0.01$ (± 0.02) mms^{-1}, the quadrupole splitting is $\Delta E_Q = (+)\ 0.29$ (± 0.02) mms^{-1} and the linewidth is $\Gamma = 0.45$ (± 0.05) mms^{-1}. (Bottom) Mössbauer spectrum of complex **13** taken at 5 K with a magnetic field of 5 T perpendicular to the γ-ray. The isomer shift is $\delta = 0.01$ (± 0.02) mms^{-1}, the quadrupole splitting is $\Delta E_Q = +\ 0.29$ (± 0.04) mms^{-1} and the linewidth is $\Gamma = 0.47$ (± 0.03) mms^{-1}.
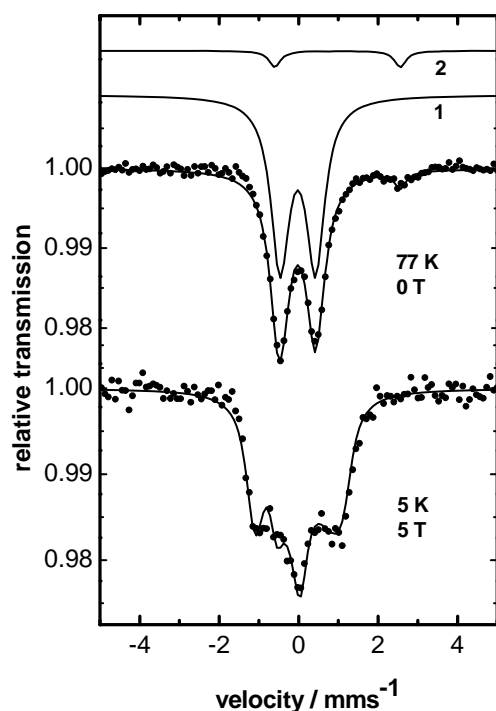
Fig. S10. (Top) Mössbauer spectrum of complex **17** taken at 77 K. There are two different components. The isomer shift for the first component is $\delta = -0.02\ (\pm 0.02)$ mms^{-1}, the quadrupole splitting is $\Delta E_Q = (+)\ 0.89\ (\pm 0.02)$ mms^{-1} and the linewidth is $\Gamma = 0.57\ (\pm 0.02)$ mms^{-1}. The relative contribution of this component is 94 %. The isomer shift for the second component is $\delta = 0.98\ (\pm 0.02)$ mms^{-1}, the quadrupole splitting is $\Delta E_Q = 3.16\ (\pm 0.02)$ mms^{-1} and the linewidth is $\Gamma = 0.35\ (\pm 0.02)$ mms^{-1}. The iron is therefore in a Fe(II) S = 2 state. The relative contribution of this component is 6 %. (Bottom) Mössbauer spectrum of complex **17** taken at 5 K with a magnetic field of 5 T perpendicular to the γ-ray. The isomer shift is $\delta = -0.01\ (\pm 0.02)$ mms^{-1}, the quadrupole splitting is $\Delta E_Q = +\ 0.91\ (\pm 0.03)$ mms^{-1} and the linewidth is $\Gamma = 0.47\ (\pm 0.02)$ mms^{-1}. The minor component splits into multiple lines at high field and is therefore not detectable under high field conditions.
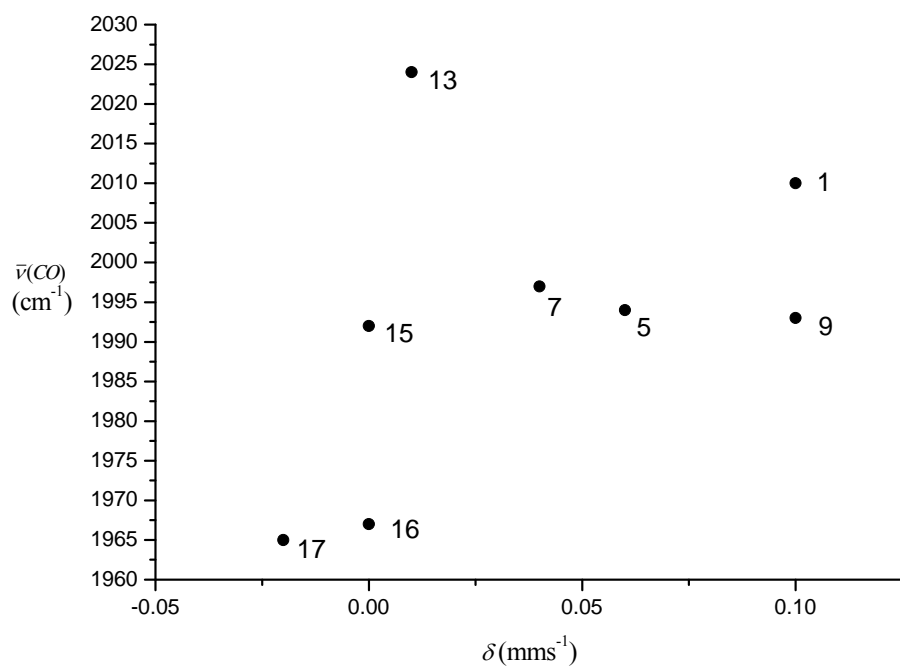
Fig. S11. Correlation of Mössbauer isomeric shifts with the averaged ν(CO) frequencies of 8 model complexes.